



Multicycle adsorption and desorption for recovery of U(VI) from aqueous solution using oxime modified zeolite-A

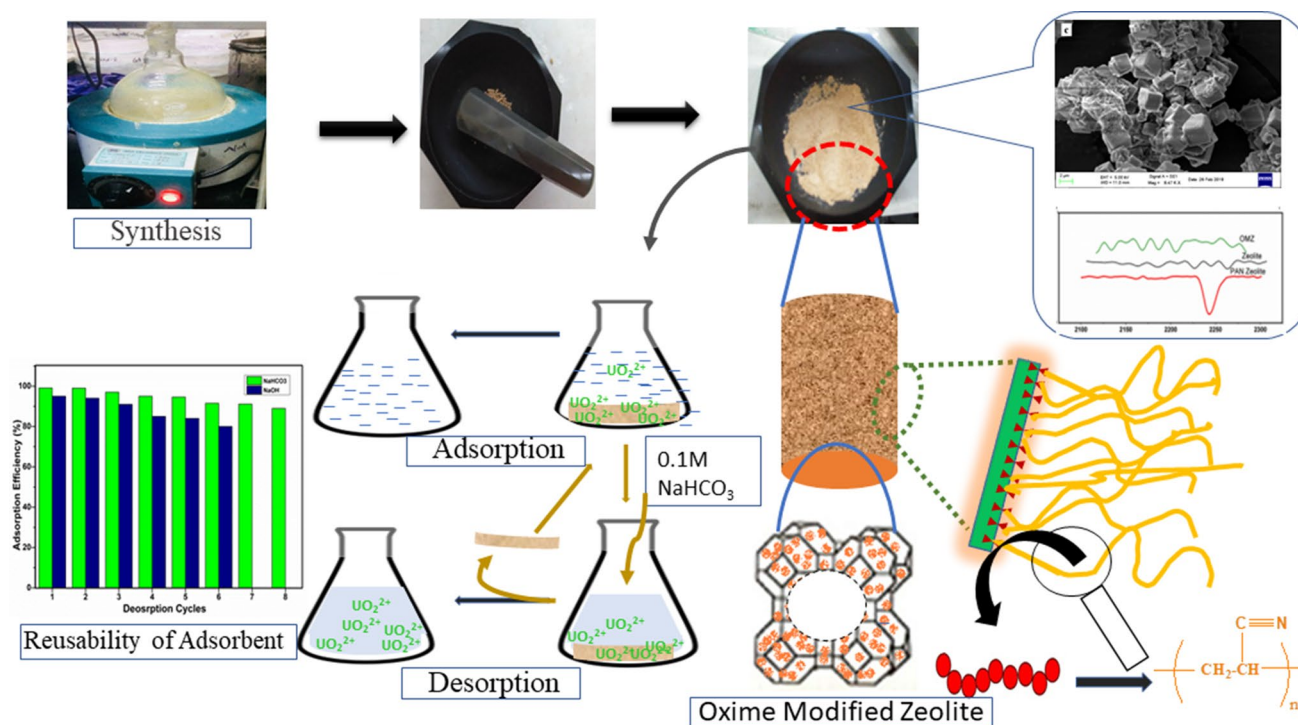
Rashmi Dahake¹ · Pratibha Tiwari¹ · Amit Bansawal¹

Received: 8 July 2020 / Accepted: 29 October 2020 / Published online: 4 January 2021
© Akadémiai Kiadó, Budapest, Hungary 2021

Abstract

This paper reports synthesis of oxime modified zeolite-A as an efficient adsorbent for uranium (U(VI)). The as prepared adsorbent was thoroughly characterised and the effect of various experimental parameters were also studied. Maximum adsorption occurs in the pH range of 4–6 with adsorption efficiency of 98%. Adsorption experiment results showed that the equilibrium data fitted well to Langmuir model and follow pseudo second order kinetics. More importantly the spent adsorbent was successfully regenerated and multicycles of adsorption and desorption were showing good efficiency in each run. The material is stable and reusable up to 8 cycles with constant adsorption efficiency. The adsorption capacity of 4.92 mg/g is observed for U(VI) in presence of other competing metal ions which include Cr, Cd, Co, Pb and Mn. It can be inferred from the results that oxime modified zeolite-A is a promising adsorbent for recovery of U(VI) due its easy separation, high adsorption and excellent reusability.

Graphic abstract



Keywords Adsorption · Zeolite · Uranium · Reusability

Extended author information available on the last page of the article

Introduction

Sources of energy are very limited and the demand for energy is increasing day by day. Nowadays nuclear energy is gaining importance as a source of clean energy [1]. However contamination caused by nuclear radiation has an adverse effect due to its theoretical mobility in water and bioaccumulation. U(VI) is widely used in the various nuclear activities. The waste of nuclear activities when disposed in the environment leads to serious poisoning of aquatic system and can also enter into the food chain [2]. Besides anthropogenic sources, U(VI) contamination may also arise from natural sources [3]. According to the recent survey, huge amount of U(VI) is present in the ground water of Panjab region (India) which may be due to local natural geology and industrial activities in the region [4]. U(VI) poses potential risk to the human health due to its radioactivity and heavy metal toxicity. Accumulation of U(VI) in kidney can introduce irreversible damage to the key filtering system in the body. The drinking water standard for U(VI) has been set to 20 ppb by United States Environmental Protection Agency (USEPA) and 15 ppb by World Health Organization (WHO) due its cancer causing activities. U(VI) is present in water under standard environmental conditions in its hexavalent form as mobile and water soluble uranyl cation ($[UO_2]^{2+}$) [5].

Different methods are available for removal and treatment of U(VI) such as chemical precipitation, solid phase extraction, ion exchange, membrane process and adsorption, etc. These methods have their own limitations such as high cost, low efficiency, large volume of waste sludge generation etc. whereas adsorption is most attractive and economic method with high potential for removal and salvaging of metal ions from water and easy operation [6]. The important role is to produce a high performance material which will be economic and is abundantly available. In the recent era scientists and researchers have developed variety of adsorption materials such as carbon based materials, inorganic clay minerals, alumina based materials, polymers, phosphate rock and biomaterials [7–12]. Among the variety of available adsorbents zeolite is more appealing due to its high exchange capacity, selectivity, well defined crystalline structure, high internal surface area, uniform pores, good thermal stability, reduced cost and strong affinity for most of the heavy metals [13]. However, adsorption capacity of natural zeolite for U(VI) is significantly low. Many researches have reported the enhancement in the adsorption capacity of zeolite by modification or functionalisation with different inorganic or organic molecules [14, 15]. Amideoxime is an amphoteric functional group which includes both oxime and amino groups on single carbon atom [16]. Due to presence of structure of

alkaline and acidic site; it shows high affinity for the various metal ions [17]. Therefore, we opted for amidoxime group for the modification of zeolite for the adsorption of U(VI) from aqueous solution.

This study involves synthesis of modified zeolite-A by grafting method and its application for the removal of uranium from water. The material is thoroughly characterized by scanning electron microscopy (SEM), X-ray diffraction, FTIR spectroscopy and elemental analysis by CHNS. The adsorption behaviour of uranium on modified zeolite are evaluated by studying pH effect, adsorption isotherm, initial concentration of uranium, contact time etc. The adsorption properties in presence of other co-existing ions have been also been conducted to study the interference due to these ions on removal efficiency.

Experimental

Chemicals and materials

All reagents used were of analytical grade. Acrylonitrile was purchased from Merck (Germany). Zeolite 5A was procured from Sigma Aldrich (India). Hydroxylamine hydrochloride, methanol, potassium per sulphate, sodium bicarbonate and sodium hydroxide were purchased from Merck (Germany). The U(VI) standard stock solution (1000 mg/L) used for the preparation of solutions was procured from Reagecon (Ireland). Type I water obtained from MilliQ deionised water system was used throughout the experiments.

Adsorbent synthesis

The adsorbent prepared in this study was synthesized by following the procedure described in the Ref. [18]. This typical procedure of synthesis consists of two step process which includes grafting of acrylonitrile on to the zeolite and functionalisation of as prepared zeolite.

Acrylonitrile was mixed with deionised water in 2:1 proportion and zeolite-A was added to the solution. Potassium persulfate was added to the mixture with continuous stirring and heating at 70 °C to initiate the polymerisation. After 4 h the mixture was allowed to cool, filtered and washed with ethanol. The as formed compound; PAN zeolite was dried in an oven for 8 h. Further functionalisation of PAN zeolite was carried out; hydroxylamine hydrochloride was added to methanol water mixture (3:1) and pH 10 was maintained by adding 1 M sodium hydroxide. PAN zeolite was added to this solution and mixture was poured into the round bottom flask equipped with condenser and magnetic stirrer bar and was kept on hot plate. After 2 h of reaction at 70 °C, the adsorbent was collected and washed with methanol–water mixture repetitively. The solution was filtered and collected

material was dried in a vacuum oven at 60 °C. The resulting material is denoted as oxime modified PAN zeolite (OMZ).

Characterization of adsorbent

The surface topography was examined using scanning electron microscopy (Carl Zeiss EVO 18, Germany). X-Ray diffraction pattern of zeolite and modified zeolite was performed using X-ray diffractometer (Rigaku Miniflex). FTIR analysis was carried for the confirmation of functional groups using FTIR Vertex 70 (Bruker, Germany). The spectra was recorded in the range of 4000–400 cm^{-1} . The CHN content was determined by using CHNS analyser (Elementar Analysensysteme GmbH, Germany). pH measurements were performed using benchtop pH meter (EUTECH Instruments).

Batch adsorption experiments

The batch adsorption experiments were conducted to examine the effect of various factors such as pH, contact time, temperature on adsorption of uranium. Concisely, OMZ was added to 100 ml uranium solution of initial concentration 1 mg/L and kept in rotary shaker at ± 120 rpm and 298 K. sodium hydroxide (3M) and hydrochloric acid (3M) solutions were used for adjustment of pH of the solution. The solution and adsorbent were separated by filtration when the adsorption equilibrium was reached. The concentration of the uranyl ion in the remaining filtered solution was analysed by Inductively Coupled Plasma Mass Spectrometer (ICP-MS) (NexION 300X, Perkin Elmer, Germany). The adsorbent was also tested using uranium spiked tap water. The adsorption amount, q_e (mg/g) of adsorbed U(VI) is calculated by Eq. 1

$$q_e = \frac{(C_0 - C_e)}{m} \times V \quad (1)$$

The specific value which is a measure of adsorbents adsorption capability called as distribution coefficient K_d is calculated by Eq. 2

$$K_d = \frac{C_0 - C_e}{C_e} \times \frac{V}{m} \quad (2)$$

where C_0 is an initial concentration of U(VI) in mg/L, C_e is an equilibrium concentration of U(VI) in mg/L, V is volume of testing solution in L and m is adsorbent dose in g.

Desorption and reusability study

Desorption studies were performed using NaHCO_3 and NaOH solution and two different set of experiments were conducted for both solutions. In each experiment, 20 mg of

the spent adsorbent was treated with 100 ml of various concentrations of NaHCO_3 and NaOH, allowed to equilibrate for 1 h, then the solution is filtered for solid liquid separation. The spent adsorbent in this study were prepared by adsorption of U(VI) solution (1 mg/L, pH 4) on 20 mg of OMZ with 100 ml for 4 h at 150 rpm and room temperature. The experimental series was repeated three times.

Results and discussion

Adsorbent characterization

Morphology and textural properties (SEM)

The SEM images were taken for characterizing the morphology of the adsorbent. Figure 1a–d are the SEM images of unmodified zeolite, PAN zeolite, OMZ and OMZ after adsorption of uranium respectively. Figure 1a shows the cubical structure with uniform dimensions and a very smooth surface of the unmodified zeolite prior to any type of modification. After the modification of zeolite by acrylonitrile followed by amidoximation, rough and uneven surface of zeolite was observed along with clusters formation which indicated grafting and functionalization of the zeolite (Fig. 1b, c). Figure 1d represent OMZ after adsorption experiment, where the intensity of clusters was denser, the surface area covered by these clusters is large and relatively smooth surface is observed compared to OMZ before adsorption.

Analysis by X-Ray diffraction (XRD)

The crystalline structure of the adsorbent was studied by XRD. Figure 2 depict the XRD patterns of unmodified zeolite-A, PAN zeolite-A, OMZ and OMZ after adsorption respectively. It was observed that even after modification of zeolite-A, the crystal structure remains identical. This shows that the zeolite exhibits morphological and chemical stability during surface functionalisation. The structure of zeolite is retained after adsorption.

FTIR analysis

The FTIR spectra were obtained for unmodified zeolite, PAN zeolite, OMZ and OMZ after adsorption represented in Fig. 3. Combined study of the three spectra shows the significant variations of functional groups corresponding to the change in each step of the reaction. The spectrum clearly shows Bathochromic shift as the obtained peaks gets shifted to higher values which governed by the increase in reduced mass indicates the loading of polymeric material over zeolite. The other reason may be the

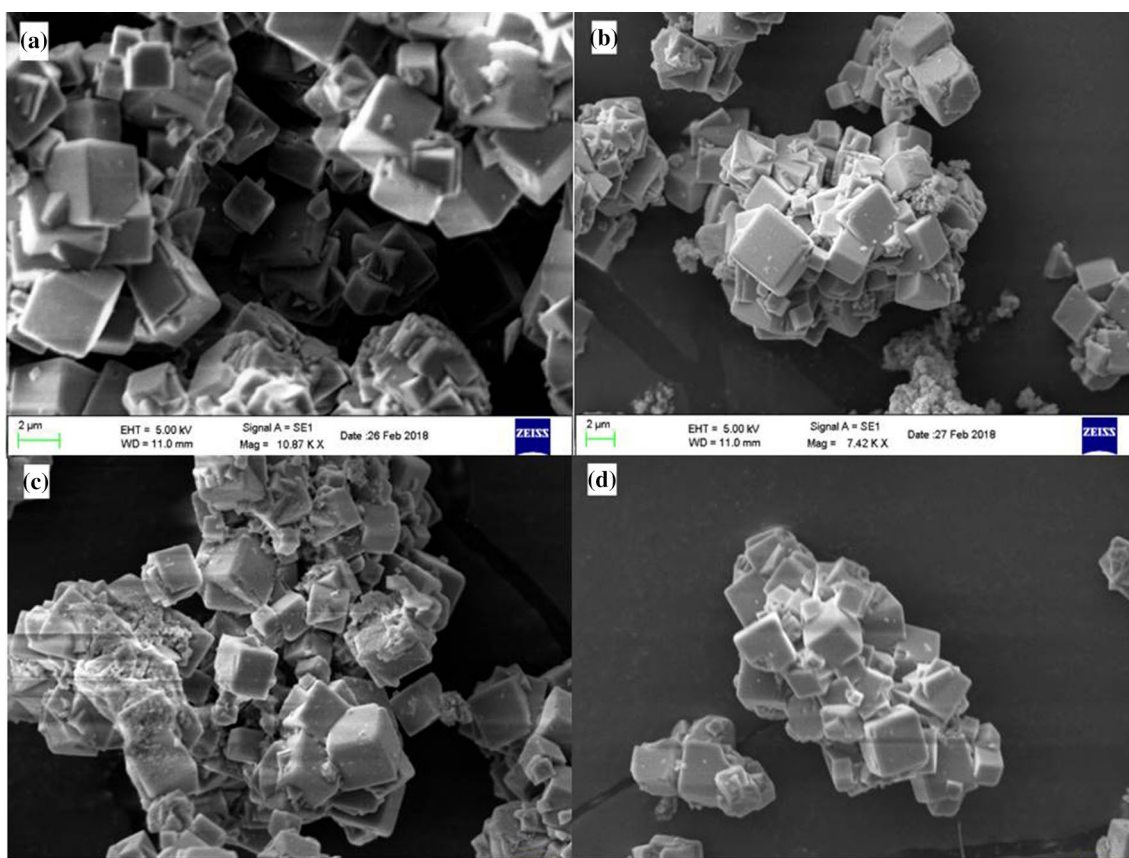


Fig. 1 SEM images of **a** unmodified zeolite **b** PAN zeolite **c** oxime modified zeolite **d** oxime modified zeolite after adsorption of uranium

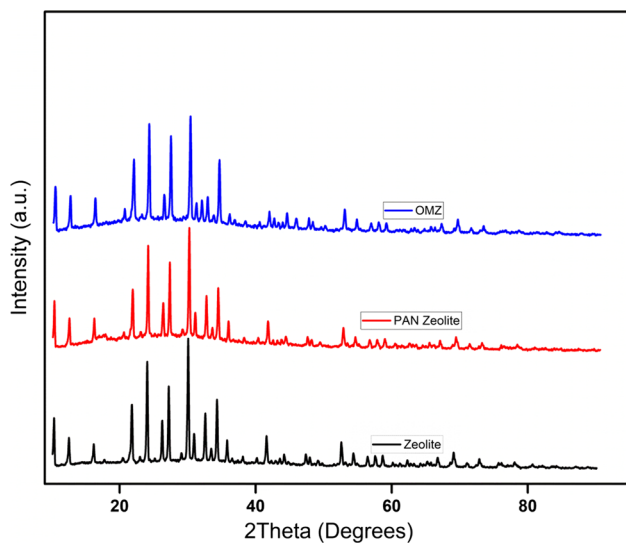


Fig. 2 XRD pattern of **a** zeolite-A **b** PAN zeolite-A **c** oxime PAN zeolite **d** OMZ after adsorption

increase in bond-lengths due to the interaction of atoms with acrylonitrile which leads to the change in electronegativity of the neighbouring atoms. The relatively greater size and inadequately observed band in the range of $3700\text{--}3500\text{ cm}^{-1}$ can be allocated to O–H stretching vibration. Moreover, the intensity of this peak is high in OMZ and seems to be decreased in its intensity due to the co-ordination of Oxygen to uranyl group. The peak at 2248 cm^{-1} observed in PAN zeolite belongs to the stretching vibration of $\text{C}\equiv\text{N}$ which disappears after amidoximation. The large band appearing at 968.52 cm^{-1} is associated to the tetrahedral arrangement of zeolite. The band at 1651 cm^{-1} found in all the spectra can be attributed to basic structure of Na–Y zeolite but the intensity of peak increased in case of OMZ which is due to the overlapping of peak for --C=N-- near 1643 cm^{-1} of oxime group. The frequency range $900\text{--}650\text{ cm}^{-1}$ represents --NH_2 group associated to bending vibration (out of the plane). [19, 20] The FTIR results confirms the formation of PAN zeolite followed by formation of oxime modified zeolite.

Fig. 3 FTIR spectra of **a** zeolite-A **b** PAN zeolite-A **c** oxime PAN zeolite **d** OMZ after adsorption

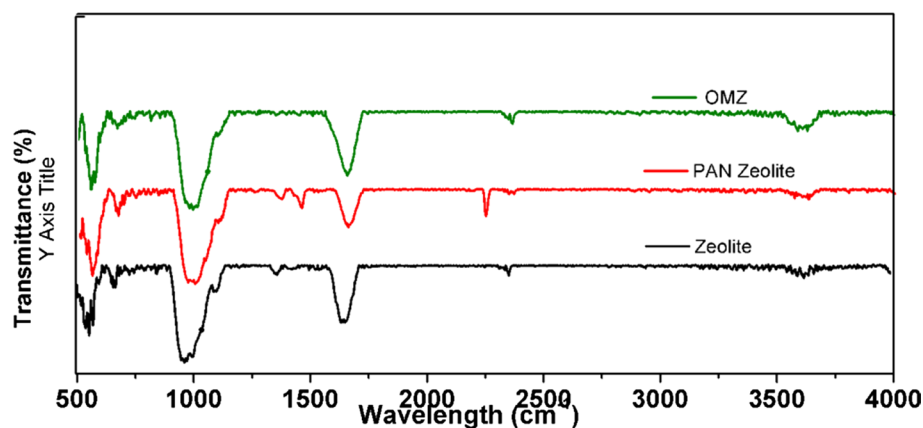


Table 1 Elemental analysis of zeolite, PAN zeolite and OMZ

Adsorbent	N (%)	C (%)	H (%)	C/N (Ratio)	C/H (Ratio)
Zeolite	0.00	0.00	1.989	0.00	0.00
PAN	4.59	11.74	0.774		
PAN zeolite	4.59	11.74	2.763	2.5548	15.16
OMZ	5.16	8.27	3.417	1.6022	7.92

Elemental analysis

Zeolite as a parent material used for grafting process does not have organic elemental contents, hence for initial affirmation of grafting, CHN analysis was done by CHNS analyser. The percentages of carbon (C), hydrogen (H) and nitrogen (N) for zeolite, PAN-zeolite and OMZ are tabulated in Table 1. Results are in good agreement with zeolite data as it shows absence of C and N. PAN as first formed material after polymerization of acrylonitrile over zeolite showed C as 11.74% which gives direct indication of grafting on zeolite polymer. In PAN-zeolite percentages of C, H, and N correspond to the organic functionalization of zeolite and the ratio of C to N obtained was 2.5548 and the ratio of C to H was 15.16 which indicates the presence of acrylonitrile polymer. In case of OMZ the C and H content decreased whereas amount of N was increased which confirms the modification of cyanide group of polymers to amideoxime group. Moreover, the ratios of C/N and C/H in OMZ correlate with functionalisation. The same observation also correlates with FTIR findings showing specific spectra at wavenumber 2248 cm^{-1} for mentioned functional groups like cyanide.

Batch adsorption studies

Effect of adsorbent dose

Effect of dose of the adsorbent on removal of U(VI) is presented in Fig. 4. It was observed that U(VI) adsorption efficiency increases with the increase in dose of adsorbent

from 0.1 to 0.75 g/L and further increase of dose does not showed any further increase in adsorption efficiency. Therefore 0.2 g/L was chosen as the optimum dose and further experiments were performed using the same dose.

Effect of pH

pH plays a vital role in the adsorption of metal on to the adsorbents. Behaviour of adsorbent at solid–liquid interfaces is greatly influenced by pH, mainly because of the interaction between change of pH and electric surface charge of adsorbent & adsorbate. Adsorption performance of OMZ was evaluated between pH 1–10 and it was observed that OMZ removes more than 80% U(VI) in wide pH range of 4–6.

U(VI) is mainly present in the form of UO_2^{+} up to the pH 6 [21, 22]. At very low pH of 2 the adsorption of U(VI) is less due to the presence of large number of H^{+} ions occupying the adsorption sites on the surface of OMZ due to which chances of adsorption of U(VI) decreases. Above pH 6 the uranium forms different complexes with OH^{-} and CO_3^{2-} which reduced the adsorption capacity of U(VI). Moreover, at $\text{pH} > 6$ complexes like $\text{UO}_2(\text{OH})_2$ starts evolving, which leads to the precipitation and hence decrease in the adsorption [23]. Also zeolite structure will collapse at pH below 4 leading to decrease in efficiency. [24] Thus maximum removal of uranium is observed at pH range of 4–6 (Fig. 5).

Adsorption kinetics

The adsorption kinetics of OMZ for U(VI) adsorption was analysed which increased sharply and reaches equilibrium within 15 min. Almost 98% of U(VI) was recovered by OMZ at initial concentration of 1 mg/L after adsorption equilibrium, which shows fast adsorption rate of OMZ for U(VI). The experimental data was simulated using pseudo first order and pseudo second order adsorption models (Fig. 6). The data was

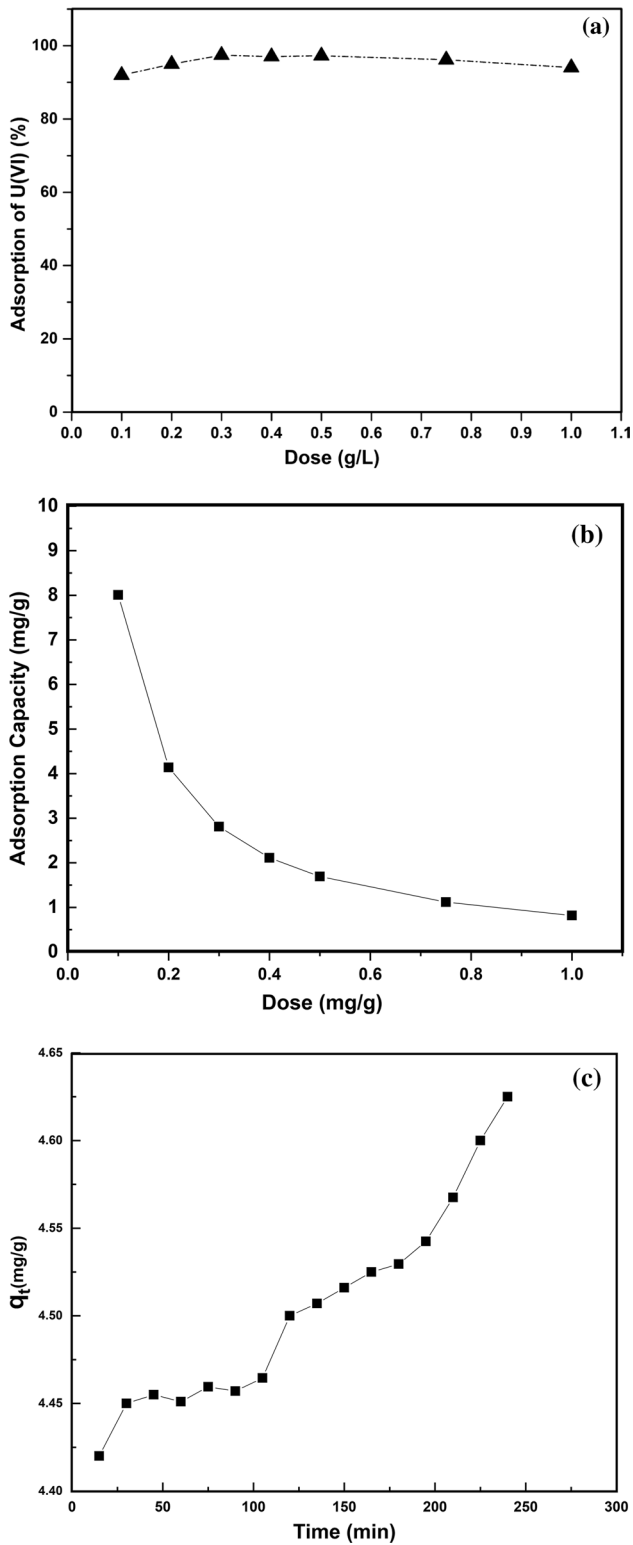


Fig. 4 **a** Effect of adsorbent dosage on adsorption of U(VI) at 298 K temperature. **b** Effect of adsorbent dosage on adsorption capacity. **c** Effect of reaction time on adsorption capacity

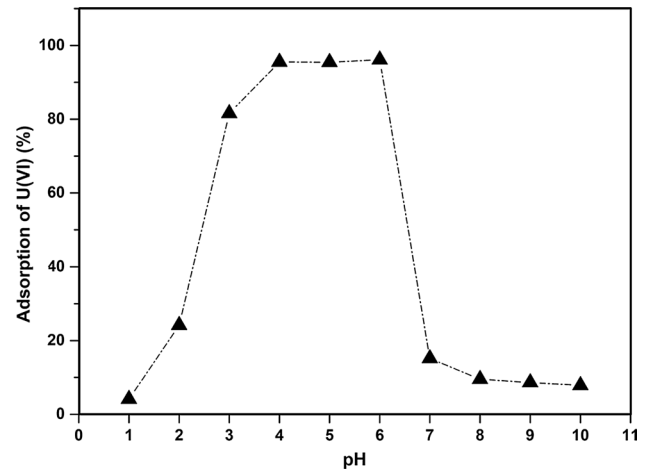


Fig. 5 Effect of pH on adsorption of U(VI) at $C_0 = 1$ mg/L and $T = 298$ K

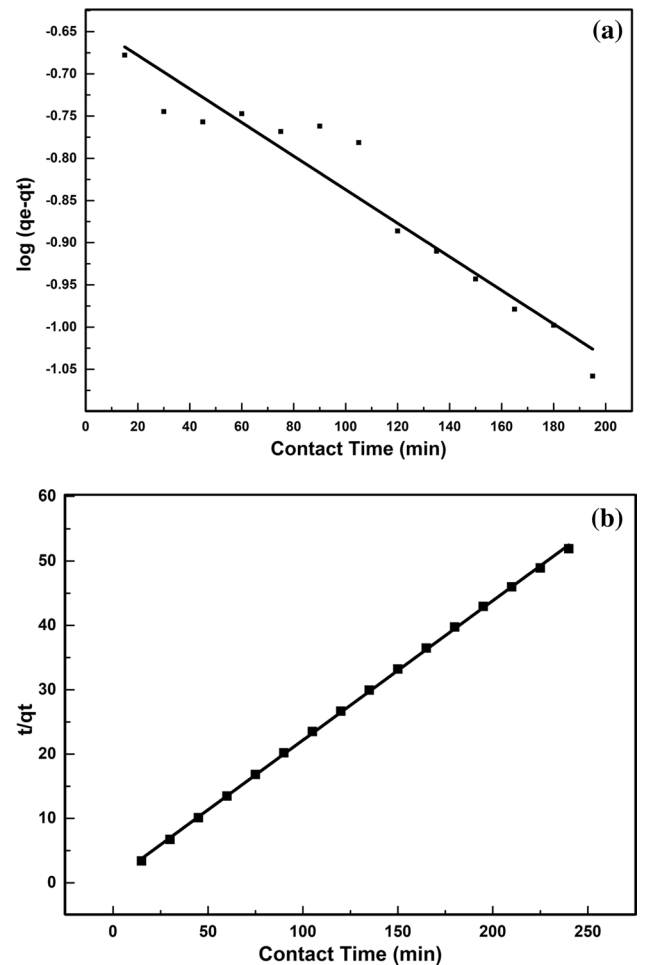
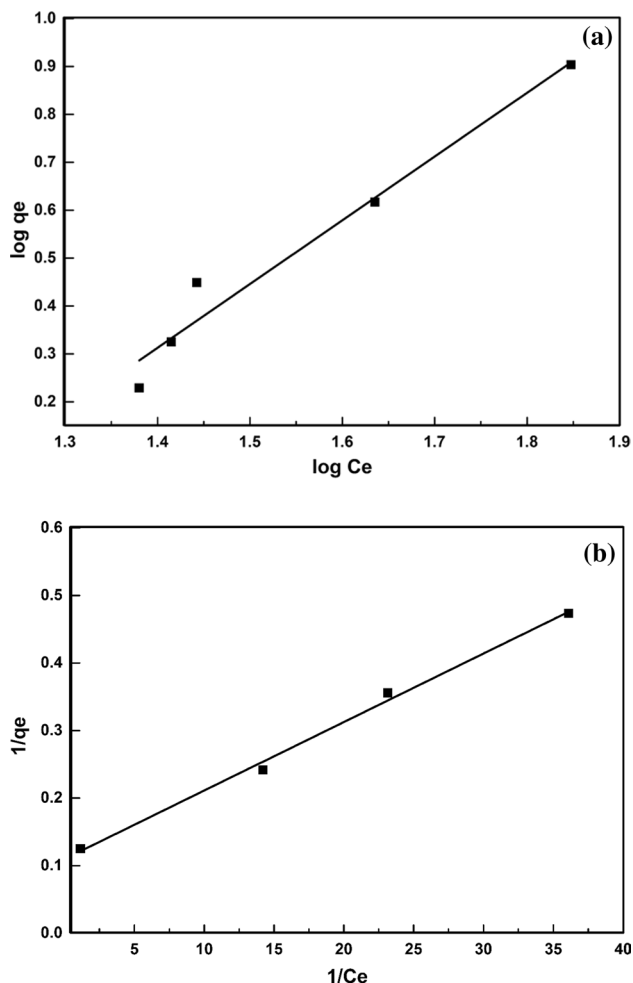


Fig. 6 **a** Pseudo first order adsorption kinetics of U(VI) over OMZ. **b** Pseudo second order adsorption kinetics of U(VI) over OMZ

Table 2 Kinetic parameters of U(VI) adsorption on OMZ

$q_{e,exp}$ (mg/g)	Pseudo first order kinetics			Pseudo first order kinetics		
	$q_{e,exp}$ (mg/g)	k_1 (min^{-1})	R^2	$q_{e,cal}$ (mg/g)	k_2 (min^{-1})	R^2
4.63	0.23	0.0046	0.93	4.616	0.089	0.999

**Fig. 7** **a** Freundlich adsorption isotherm (pH=4, $C_0=1$ mg/L, Temperature=298 K). **b** Langmuir adsorption isotherm (pH=4, $C_0=1$ mg/L, Temperature=298 K)

in good agreement with pseudo second order kinetic model with correlation coefficient of 0.999 as compared to pseudo first order kinetics, details of which are listed in Table 2. The assumption used for the pseudo second order kinetics is that the rate determining step is chemical adsorption. The obtained results indicate that the adsorption behaviour involves sharing

and replacing of electrons between U(VI) and OMZ through valence forces i.e. chemisorption.

Adsorption isotherms

The adsorption isotherms were obtained by varying the dose of adsorbent from 0.1 to 0.75 g/L at constant temperature (298 K) and initial concentration (1 mg/L) as represented in Fig. 7a, b. For analysis of equilibrium data Langmuir and Freundlich adsorption isotherm models were selected. The slope and the intercept line equation provided correlation coefficient and corresponding constant which are listed in the Table 3. Excellent fit with correlation coefficient of 0.995 was obtained after plotting the U(VI) adsorption data for Langmuir isotherm model. This represents that the adsorption of U(VI) occur on the surface of the OMZ. The calculated value of adsorption capacity (q_e) is closely matching with the value obtained experimentally.

Effect of presence of competing ions and coexisting ions

The experiments were also performed to understand the effect of other co-existing and competing ions as depicted in Fig. 8a. Co-ion study plays a major role in describing the interferences and its effect on adsorption. The aqueous uranium solution was spiked with different ions such as sodium, calcium, potassium, magnesium and ammonium ions keeping adsorbent dose constant to 0.2 g/L. The systems were kept for agitation for 4 h for the maximum adsorption. Results obtained indicate no significant effect on adsorption efficiency in presence of other ions. This study shows higher selectivity of synthesized adsorbent (OMZ) towards uranium.

Figure 8b shows comparison of adsorption efficiencies of various metal ions on OMZ at pH 4. It is observed that the adsorption capacity of U(VI) (4.92 mg/g) is significantly higher than the other ions such as Cr(3.38 mg/g), Cd(3.21 mg/g), Co(2.93 mg/g), Pb(3.75 mg/g), Mn(2.94 mg/g). These results explained that OMZ have more effective enrichment for U(VI) compared to other metals.

Table 3 Parameters of Langmuir and Freundlich isotherm for adsorption of U(VI) adsorption on OMZ

Adsorbent	Langmuir adsorption isotherm			Freundlich adsorption isotherm		
	K_L	q_m	R^2	K_F	N	R^2
OMZ	10.9	9.1743	0.996	0.042	0.811	0.975

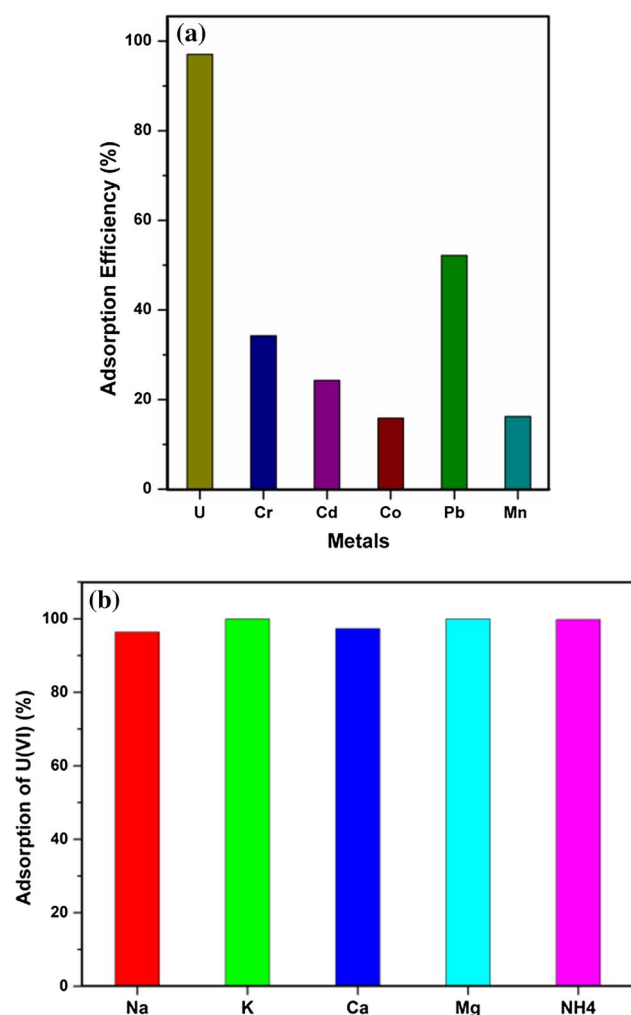


Fig. 8 a Competitive adsorption efficiency of OMZ for U(VI) over competing ions. b Competitive adsorption efficiency of OMZ for coexisting ions

Desorption and reusability

The potential of the adsorbent material is majorly evaluated on the basis of reusability of the material. It is required that the adsorbent should retain the original adsorption performance after several cycles of desorption. It is accepted that strong acidic medium can strip of U(VI) but can damage the structure of adsorbent or its active sites [25]. From the pH study it was observed that maximum adsorption efficiency was obtained at lower pH. Thus, pH was increased for desorption of U(VI) ions. pH can be increased by using basic salts like sodium hydroxide, sodium carbonate, sodium bicarbonate etc. In order to evaluate desorption behaviour of OMZ the spent adsorbent was treated with 100 mM sodium bicarbonate and 10 mM NaOH for 1 h at room temperature. Consecutively adsorption and desorption cycles were performed for 8 times using 100 mM NaHCO₃ and 6 times

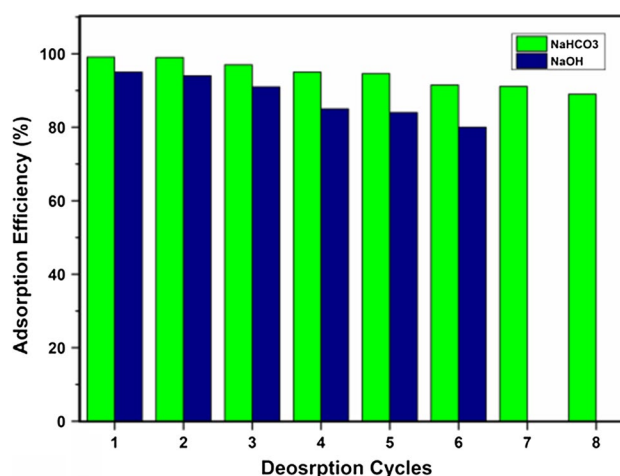


Fig. 9 Reusability of OMZ for removal of U(VI)

using 10 mM NaOH with same adsorbent and using freshly prepared U(VI) solution (1 mg/L). Adsorption efficiency of 90% and 80% even after 8th cycle of NaHCO₃ and 6th cycle of NaOH treatment was observed respectively (Fig. 9).

Adsorption mechanism

Zeolite A is a synthetic sodium aluminium silicate with the formula Na₁₂ [(AlO₂)₁₂(SiO₂)₁₂] · 27H₂O. Due to the excellent properties of zeolite A, as high surface area porous material with surface functionality [26]. In the first step when zeolite A is treated with acrylonitrile, a layer of polyacrylonitrile is grafted on zeolite A; the new product formed is called PAN zeolite. In the second step when PAN zeolite is treated with hydroxylamine hydrochloride leads to the formation of amidoxime PAN zeolite called OMZ (oxime modified zeolite). When this product (OMZ) comes in contact with U(VI), the nitrogen and oxygen groups present in OMZ forms a complex with uranium [27]. Initially the adsorption studies were performed with unmodified zeolite which shows approximately 50% removal and after functionalisation with oxime removal efficiency increases to 98%. This indirectly indicate that the nitrogen and oxygen groups present in oxime plays significant role. Further, the formation of complex between uranium and oxime with electron donating sites namely oxygen and nitrogen is well established (Fig. 10).

U(VI) forms a coordinate complex, involving hydroxyl group and amino group from amidoxime motif present on OMZ which was evident from the FTIR results. U(VI) acts as metal ion and nitrogen, oxygen both having lone pair of electron acts as ligand, forming metal–ligand bidentate uranium complex [28, 29].

Considering FTIR spectra of oxime modified zeolite (OMZ) and residual uranium, the frequency range

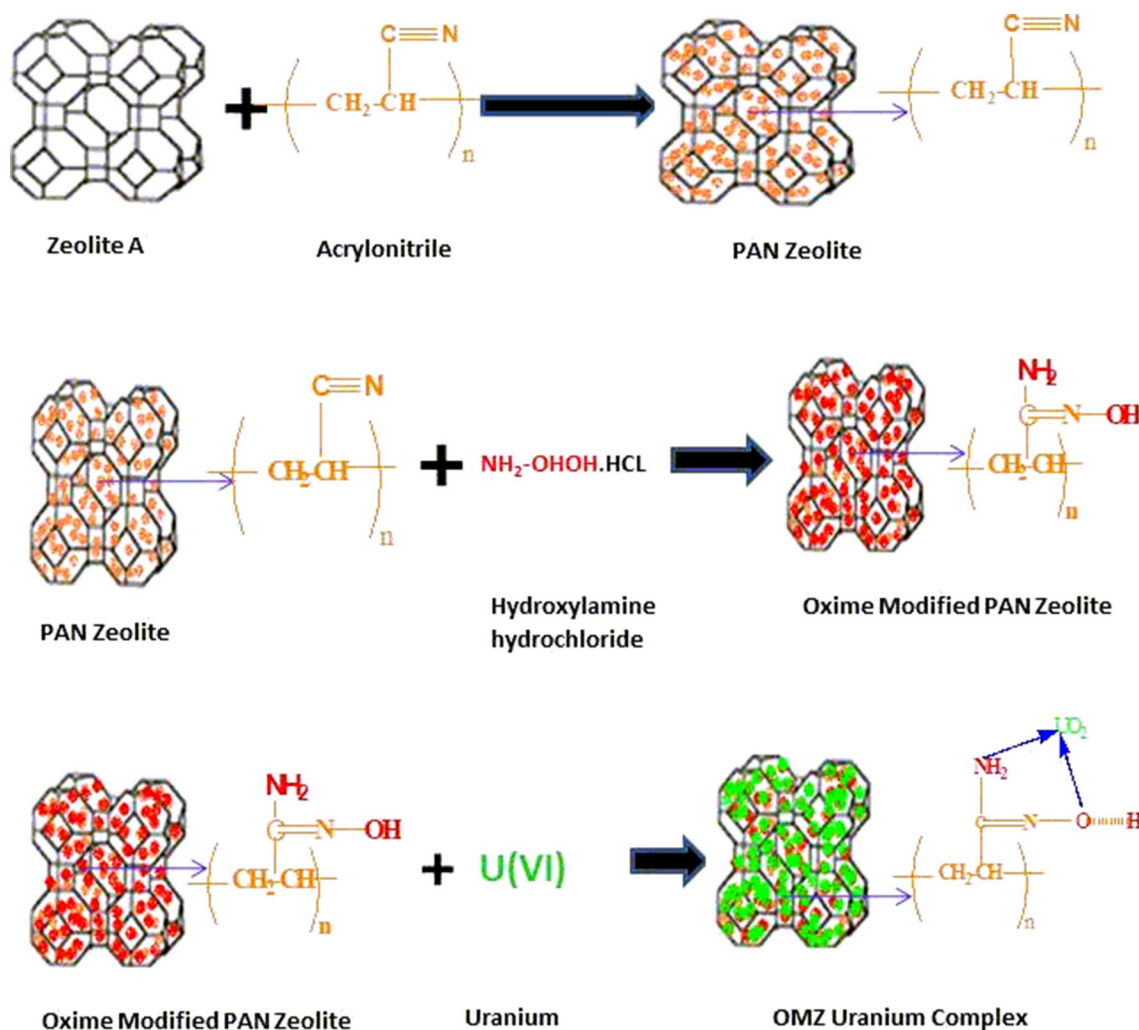


Fig. 10 Mechanism diagrams

3700–3500 cm⁻¹ corresponds to the presence of O–H group. This O–H peak is observed in both OMZ and residual uranium, but in the residual uranium there is a change in intensity of O–H peak. The intensity of O–H group in OMZ is much higher as compared to that of residual uranium indicating involvement of O–H group in the adsorption process.

Moreover, frequency range of 900–650 cm⁻¹ represents –NH₂ group associated with bending vibration. The –NH₂ group peak was also observed in OMZ but it was absent in uranium saturated OMZ indicating the interaction of –NH₂ in coordination with Uranium.

Conclusions

Polyamidoxime modified zeolite-A is first time reported for the adsorption of U(VI). The zeolite- A is modified by polymerisation followed by grafting of amidoxime group.

OMZ shows high efficiency of up to 98% for the adsorption of U(VI). The adsorption reaches equilibrium within 5 min with adsorption capacity of 4.6 mg U/g. The adsorbent is showing high efficiency of about 90% after 8 cycles of adsorption and desorption. The adsorbent is highly efficient in the pH range of 4–6 and in presence of other competing ions.

References

1. Brook BW, Alonso A, Meneley DA et al (2014) Why nuclear energy is sustainable and has to be part of the energy mix. *Sustain Mater Technol* 1:8–16. <https://doi.org/10.1016/j.susmat.2014.11.001>
2. Burns PC, Ewing RC, Navrotsky A (2012) Nuclear fuel in a reactor accident. *Science* 80(335):1184–1188. <https://doi.org/10.1126/science.1211285>

3. Waseem A, Ullah H, Rauf MK, Ahmad I (2015) Distribution of natural uranium in surface and groundwater resources: a review. *Crit Rev Environ Sci Technol* 45:2391–2423. <https://doi.org/10.1080/10643389.2015.1025642>
4. Bajwa BS, Kumar S, Singh S et al (2017) Uranium and other heavy toxic elements distribution in the drinking water samples of SW-Punjab, India. *J Radiat Res Appl Sci* 10:13–19. <https://doi.org/10.1016/j.jrras.2015.01.002>
5. Quality D (2005) Uranium in drinking-water
6. Katsoyiannis IA, Zouboulis AI (2013) Removal of uranium from contaminated drinking water: a mini review of available treatment methods. *Desalin Water Treat* 51:2915–2925. <https://doi.org/10.1080/19443994.2012.748300>
7. Sun Y, Wu ZY, Wang X et al (2016) Macroscopic and microscopic investigation of U(VI) and Eu(III) adsorption on carbonaceous nanofibers. *Environ Sci Technol* 50:4459–4467. <https://doi.org/10.1021/acs.est.6b00058>
8. Abubakar M, Tamin MN, Saleh MA et al (2016) Preparation and characterization of a nigerian mesoporous clay-based membrane for uranium removal from underground water. *Ceram Int* 42:8212–8220. <https://doi.org/10.1016/j.ceramint.2016.02.031>
9. Ren B, Fan M, Tan L et al (2016) Electrospinning synthesis of porous Al₂O₃ nanofibers by pluronic P123 triblock copolymer surfactant and properties of uranium (VI)-sorption. *Mater Chem Phys* 177:190–197. <https://doi.org/10.1016/j.matchemphys.2016.04.017>
10. Oyola Y, Dai S (2016) High surface-area amidoxime-based polymer fibers co-grafted with various acid monomers yielding increased adsorption capacity for the extraction of uranium from seawater. *Dalt Trans* 45:8824–8834. <https://doi.org/10.1039/c6dt01114d>
11. Wang R, Ye J, Ning G et al (2016) Microwave-assisted rapid synthesis of cerium phosphates and their adsorption on uranium(VI). *Res Chem Intermed* 42:5013–5025. <https://doi.org/10.1007/s11164-015-2342-5>
12. Mustafa J, Kausar A, Bhatti HN, Ilyas S (2016) Sequestering of uranium(VI) onto eucalyptus bark: kinetic, equilibrium and thermodynamic studies. *Desalin Water Treat* 57:14578–14589. <https://doi.org/10.1080/19443994.2015.1065443>
13. Olmez Aytas S, Akyil S, Eral M (2004) Adsorption and thermodynamic behavior of uranium on natural zeolite. *J Radioanal Nucl Chem* 260:119–125. <https://doi.org/10.1023/B:JRNC.0000027070.25215.92>
14. Matijasevic S, Zildzovic S, Stojanovic J et al (2016) Removal of uranium(VI) from aqueous solution by acid modified zeolites. *Zast Mater* 57:551–558. <https://doi.org/10.5937/zasmat1604551m>
15. Nekhunguni PM, Tavengwa NT, Tutu H (2017) Sorption of uranium(VI) onto hydrous ferric oxide-modified zeolite: assessment of the effect of pH, contact time, temperature, selected cations and anions on sorbent interactions. *J Environ Manage* 204:571–582. <https://doi.org/10.1016/j.jenvman.2017.09.034>
16. Liu F, Xiong W, Liu J et al (2018) Novel amino-functionalized carbon material derived from metal organic framework: a characteristic adsorbent for U(VI) removal from aqueous environment. *Colloids Surf A Physicochem Eng Asp* 556:72–80. <https://doi.org/10.1016/j.colsurfa.2018.08.009>
17. Zheng Z, Wang Y, Zhao W et al (2017) Adsorptive removal of uranyl ions in aqueous solution using hydrothermal carbon spheres functionalized with 4-aminoacetophenone oxime group. *J Radioanal Nucl Chem* 312:187–198. <https://doi.org/10.1007/s10967-017-5209-y>
18. Elwakeel KZ, El-Bindary AA, Kouta EY, Guibal E (2018) Functionalization of polyacrylonitrile/Na-Y-zeolite composite with amidoxime groups for the sorption of Cu(II), Cd(II) and Pb(II) metal ions. *Chem Eng J* 332:727–736. <https://doi.org/10.1016/j.cej.2017.09.091>
19. Akl ZF, El-Saeed SM, Atta AM (2016) In-situ synthesis of magnetite acrylamide amino-amidoxime nanocomposite adsorbent for highly efficient sorption of U(VI) ions. *J Ind Eng Chem* 34:105–116. <https://doi.org/10.1016/j.jiec.2015.10.042>
20. Yan J, Li Y, Li H et al (2019) Effective removal of ruthenium (III) ions from wastewater by amidoxime modified zeolite X. *Microchem J* 145:287–294. <https://doi.org/10.1016/j.microc.2018.10.047>
21. Abhilash Pandey BD (2013) Microbially assisted leaching of uranium—a review. *Miner Process Extr Metall Rev* 34:81–113. <https://doi.org/10.1080/08827508.2011.635731>
22. Kumar A, Tripathi RM, Rout S et al (2014) Characterization of groundwater composition in Punjab state with special emphasis on uranium content, speciation and mobility. *Radiochim Acta* 102:239–254. <https://doi.org/10.1515/ract-2014-2109>
23. Wei X, Liu Q, Zhang H et al (2017) Efficient removal of uranium(VI) from simulated seawater using amidoximated polyacrylonitrile/FeOOH composites. *Dalt Trans* 46:15746–15756. <https://doi.org/10.1039/c7dt02164j>
24. Kim JS, Zhang L, Keane MA (2001) Removal of iron from aqueous solutions by ion exchange with Na-Y zeolite. *Sep Sci Technol* 36:1509–1525. <https://doi.org/10.1081/SS-100103885>
25. Yang Z, Peng H, Wang W, Liu T (2010) Crystallization behavior of poly(ϵ -caprolactone)/layered double hydroxide nanocomposites. *J Appl Polym Sci* 116:2658–2667. <https://doi.org/10.1002/app>
26. Flanigen EM (2001) Chapter 2 Zeolites and molecular sieves: an historical perspective. In: van Bekkum H, Flanigen EM, Jacobs PA, Jansen JC (eds) *Introduction to zeolite science and practice*. Elsevier, Amsterdam, pp 11–35
27. Tsantis ST, Zagoraiou E, Savvidou A et al (2016) Binding of oxime group to uranyl ion. *Dalt Trans* 45:9307–9319. <https://doi.org/10.1039/c6dt01293k>
28. Zhao Y, Li J, Zhang S, Wang X (2014) Amidoxime-functionalized magnetic mesoporous silica for selective sorption of U(VI). *RSC Adv* 4:32710–32717. <https://doi.org/10.1039/c4ra05128a>
29. Ji G, Zhu G, Wang X et al (2017) Preparation of amidoxime functionalized SBA-15 with platelet shape and adsorption property of U(VI). *Sep Purif Technol* 174:455–465. <https://doi.org/10.1016/j.seppur.2016.10.048>

Publisher's Note Springer Nature remains neutral with regard to jurisdictional claims in published maps and institutional affiliations.

Affiliations

Rashmi Dahake¹ · Pratibha Tiwari¹ · Amit Bansiwali¹ 

✉ Amit Bansiwali
ak_bansiwali@neeri.res.in

¹ CSIR- National Environmental Engineering Research Institute, Nagpur, India